Indian J. Genet., (2023); 83(1): 52-58
doi: 10.31742/ISGPB.83.1.7

ISSN: 0975-6906
www.ijgpb.org

RESEARCH ARTICLE

Comparative transcriptome analysis of wheat isogenic lines provides insights into genes and pathways associated with stripe rust resistance

Parinita Das, Monendra Grover, Divya Chauhan, D. C. Mishra, Sundeep Kumar[1], Krishna K. Chaturvedi, Subhash C. Bhardwaj[2], Amit Kumar Singh[1]* and Anil Rai

Abstract

Stripe rust of wheat, caused by *Puccinia striiformis* f. sp. *tritici* (*Pst*) is one of the major biotic stress factors limiting wheat production worldwide. Despite the efficiency of fungicide treatments, genetic resistance is considered to be the most economical and environment-friendly way to control the disease. To study the early defense response induced by *P. striiformis* infection, RNA-seq was conducted between stripe rust-resistant and susceptible lines (FLW29, PBW343) under *Pst*-treated and control conditions. Seedlings of both genotypes were infected with pathotype 46S119, and leaf samples were collected at 12 hpi, 48 hpi, and 72 hpi. A total of 486 and 409 transcripts were differentially expressed respectively from both inoculated and mock inoculated samples. The identified DEGs comprised of defense-related genes such as WRKY, MYB, NAC transcriptional factors; PR proteins, MAPKs and serine/threonine-protein kinase signaling pathways. Further, the protein-protein Interaction (PPI) network was constructed and visualized, which will serve to identify regulatory relationships of the proteins encoded by the DEGs. The whole transcriptome sequencing study suggested key genes which can be further explored to understand the molecular mechanisms controlling stripe rust resistance in wheat.

Keywords: Wheat, Transcriptome analysis, Differentially expressed genes , Pathways, RNAseq, Biotic stress.

Introduction

Bread wheat (*Triticum aestivum* L.) (2n=42), belongs to the Poaceae family, and is one of the most important cereal grain and staple food crops around the world. It is the largest volume crop traded internationally and grown on approximately 17% of the world's cultivatable land (Gupta et al. 2009). The global demand of wheat is gradually increasing, but biotic and abiotic stresses are important factors limiting wheat production and grain quality.

Among different biotic stresses, stripe rust caused by *Puccinia striiformis* f. sp. *tritici* (Pst) is one of the most destructive fungal diseases of bread wheat, affecting especially in cool temperate and humid environments, causing significant yield losses in the major wheat producing countries (Chen et al. 2014). It causes decrease in seed vigour leading to shriveled grains, loss in number of grains per spike and thousand grain weight. The yield loss due to this disease can range from 10–70% to complete crop failure (Chen 2005). Although agricultural chemicals also protect against stripe rust, breeding resistant cultivars is the most effective, economic, and environmentally favorable method for controlling diseases (Dodds and Rathjen 2010). To date, more than 80 wheat stripe rust-resistance (*Yr*) genes have been discovered, and 40 of them have been temporarily named (Wabila et al. 2019). Cappella desprez (CD) cultivar is known as a carrier of rust resistance genes in wheat

ICAR-Indian Agricultural Statistics Research Institute, New Delhi 110 012 Delhi, India

[1]ICAR-National Bureau of Plant Genetic Resources, New Delhi 110 012, India

[2]ICAR-Indian Institute of Wheat and Barley Research, Flowerdale, Shimla 171002 Himachal Pradesh, India

***Corresponding Author:** Amit Kumar Singh, ICAR-National Bureau of Plant Genetic Resources, New Delhi 110 012, India, E-Mail: amit.singh5@icar.gov.in

How to cite this article: Das P., Grover M., Chauhan D., Mishra D.C., Kumar S., Chaturvedi K.K., Bhardwaj S.C., Singh A.K. and Rai A. 2023. Comparative transcriptome analysis of wheat isogenic lines provides insights into genes and pathways associated with stripe rust resistance. Indian J. Genet. Plant Breed., **83**(1): 52-57.

Source of support: ICAR-NBPGR, GOI, New Delhi.

Conflict of interest: None.

Received: Nov. 2022 **Revised:** Jan. 2023 **Accepted:** Feb. 2023

© The Author(s). 2023 Open Access This article is Published by the Indian Society of Genetics & Plant Breeding, NASC Complex, IARI P.O., Pusa Campus, New Delhi 110012; Online management by www.isgpb.org

against stripe rust disease. CD also possesses many *Yr* genes, including *Yr16*, a gene conferring adult plant resistance to stripe rust (Pawar et al. 2016).

The majority of molecular analyses of host pathogen interactions have been restricted to a limited number of genes, but with the advances in sequencing technologies, it has become affordable to study the complete transcriptome of the host as well as a pathogen. In order to have a complete understanding of genes and pathways associated with the wheat–stripe rust resistance, the knowledge of the whole set of genes differentially expressed at various stages of host-pathogen interactions is crucial. Therefore, RNA-seq analysis was carried out in the present investigation for stripe rust susceptible cultivar PBW343 and its resistant NIL FLW29 differing for *Yr16* to discover putative candidate genes and signaling pathways underlying the defense mechanism against stripe rust.

Materials and methods

Plant material and collection of samples

Common wheat (*T. aestivum*) cultivar, PBW343 (susceptible) and its NIL FLW29 (resistant) with resistance gene *Yr16* were used in this study. Leaf samples were collected from both the genotypes at the seedling stage under control and biotic stress (stripe) treatment *i.e., Pst* 46S119 pathotype and at three time points, 12, 48 and 72 hours after inoculation. Three replicates were collected for each line at each time points.

RNA extraction, library construction, and sequencing

Total RNA was isolated from *Pst* treated and mock-inoculated leaf samples using Qiagen RNeasy Mini kit (Qiagen Inc, USA) using according to the manufacturer's instruction, including the recommended treatment with DNase. RNA 6000 Nano Kit on a 2100 Bioanalyzer was used to verify the quality of the total RNA (Agilent Technologies, USA). RNA concentrations were determined with a NanoDrop ND-8000 spectrophotometer. cDNA libraries were constructed using IlluminaTrueSeq RNA library preparation kit, according to manufacturers recommended protocol and sequencing was carried out on single HiSEQ 4000 lane using 150 bp paired-end chemistry. The commercial service provider handled the library preparation and sequencing (NxGenBio Life Sciences, New Delhi, India).

Analysis of RNA-seq data

The quality of raw sequence generated from Illumina Hiseq 4000 platform were checked using FASTQC tool (Andrews 2010). Clean reads were obtained by removing the low-quality reads, cleaning of the data and removing adapters using Trimmomatic tool (Bolger et al. 2014) keeping phred-score > 30. The clean reads were mapped to the wheat reference genome, RefSeqv1.0 (IWGSC, 2018) using TopHat (Trapnell et al. 2009) and Cufflinks (Trapnell et al. 2010) tool which performed reference-based transcriptome assembly. Expression values of the transcripts were calculated in the form of fragments per kilobase of exon per million mapped reads (FPKM) values. Further, these expression values were compared between PBW343 and FLW29 lines for both control and treated condition at each time points by Cuffdiff tool in the form of log (fold change) value. After getting the differential expression values. The DEGs were visualized by a R package, CummeRbund (Goff et al. 2012).

Gene annotation and pathway analysis

Homology search of differentially expressed genes (DEGs) from different time points were subjected to blast against NCBI non-redundant database (ftp://ftp.ncbi.nlm.nih.gov/blast/db/) using Blastx algorithm as standalone local NCBI-blast-2.2.31+ with threshold E-value 1e-3 (Altschul et al. 1990). Further Blast2GO tool (https://www.blast2go.com/) (Conesa et al. 2005) was used for mapping, annotation and interproscan of DEGs. The functional classification was done using the Gene Ontology (GO) and Kyoto Encyclopedia of Genes and Genomes (KEGG) databases (Kanehisa and Goto, 2000) for broader overview of the crop species and the pathways involved. The Gene Ontology (GO) graph of DEGs between the NILs was generated using the WEGO program (Ye et al. 2006). Genes were functionally categorized into three sub-categories: biological process, molecular function and cellular component. Blastx was performed against PlantTFDB 4.0 (http://planttfdb.cbi.pku.edu.cn/download.php) (Jin et al. 2017) for finding out transcriptional factors in DEGs. Further, Mapman pathway analysis (version 3.5.1; http://mapman.gabipd.org/web/guest) (Thimm et al. 2004) was done to decipher the biotic stress-responsive pathways in which the DEGs were involved with a p-value limit of ≤ 0.05.

Protein-protein interaction network construction

Using the online STRING (http://string-db.org/) database (Franceschini et al. 2013), we developed a network of DEG-encoded proteins and their interactions with a score ≥0.7. Further, Cytoscape software (Shannon et al. 2003) was applied to visualize the protein interaction relationship network and analyze hub proteins, with having important nodes with many interactions.

RNA-seq data submission

The raw data used in the present study for transcriptome assembly and gene expression analysis have been submitted to the NCBI Sequence Read Archive (SRA) bio project under accession number PRJNA613349.

Results and discussion

Generation of RNA-seq data and transcriptome assembly

After stringent quality check and data cleaning, 611.723838

million high quality reads were obtained. The quality index Q20 was nearly 96–97% and the overall average GC content was about 55%, indicating good input reading quality (Supplementary Table S1). Utilizing these cleaned reads from 36 RNA-seq datasets, a reference-based transcriptome assembly was generated using program Tophat. The alignment statistics of FLW29 and PBW343 (Supplementary Table S2) shows that the reads are aligned to the reference genome on an average of 75–80% for both lines. Merging the several Cufflinks assemblies together using Cuffmerge, a total of 164095 transcripts were generated and the number and length distribution of the transcripts were shown in Supplementary Fig. S1.

Abundance estimation and identification of DEGs

With threshold value of absolute log2 (fold change) ≥2 (upregulated) and ≤ -2 (downregulated) and P-value ≤ 0.05, putative DEGs were identified based on 6 biologically pairwise comparison (Table 1). The total number of DEGs for *Pst* treated sample (486 DEGs) were found higher than the controlled samples (409 DEGs).

The results from Venn diagram showed only 6 overlapping DEGs from the control samples of 12, 48 and 72 hours. Whereas, a number of 83, 54 and 138 DEGs were unique at 12, 48 and 72 hours, respectively. In case of *Pst* inoculated samples 7 overlapping DEGs were found and number of unique genes were 74, 188 and 65 for 12, 48 and 72 hpi, respectively (Fig. 1). The expression of upregulated genes was highest at 48 hpi and the downregulated genes were expressed highest at 72hpi. The Volcano plots were used to visualize the number of significant transcripts across the time duration (Supplementary Fig. S2). The heatmap of top 30 DEGs from both line were used to compare their expression across the time points (Supplementary Fig. S3).

Annotation of DEGs and identification of R genes

Blastx results showed that 88, 251 and 128 DEGs having similarities with other existing genes in the nr-database at 12, 48 and 72 hpi, respectively. Top hit species distribution of *Pst* treated DEGs revealed maximum hits with *Triticum turgidum* subsp. durum, followed by *Aegilops tauschii* subsp. *tauschii, T. aestivum, Triticum uratu* and *Hordium vulgare*. We observed variable expression of disease resistance-associated R genes across time points. More number of R genes displayed differential expression at 48 and 72 hpi than at 12 hpi. Among the key R genes that were upregulated at 48 hpi include disease resistance protein RPM-like 1, leaf rust 10 disease-resistance protein, serine/threonine-protein kinase-like protein CCR3, STY46 and PBL28. The upregulation of these genes in FLW29, suggests their likely role in imparting resistance against *Pst*. Several PR proteins, such as thaumatin-like protein TLP7, pathogenesis-related protein 1-18, catonic peroxidase, mitogen-activated protein kinase were upregulated in resistant genotype FLW29 during the resistance response and may enable it survive against the *Pst* infection (Zhang et al. 2020).

Gene ontology based functional analysis of the DEGs

The GO annotations results revealed that cellular process (32.05%) was the largest group under the biological process category, followed by the metabolic process (32.01%). Under the cellular component category, cytoplasm (18%), membrane (14%) and organelle (14%) were the largest groups, whereas in the molecular function category, ion binding (16%), organic cyclic compound binding (15%) and heterocyclic compound binding (15%) was the largest group, followed by catalytic activity (13%). These similar aforementioned results showed that normal biological activity was dependent on the regulation of biological processes, which has also been observed in tissues of various species in response to infection (Wang et al. 2009)(Supplementary Fig. S4; Fig. 2).

KEGG pathway classification of DEGs

The KEGG pathway analysis showed that the genes of "phenylpropanoid biosynthesis" pathway were highly enriched at all three-time points. Secondary metabolic compounds such as SA, lignins, flavonoids, phytoalexins and coumarins produced by the phenylpropanoid pathway, play important roles in plant systemic resistance (Weisshaar and Jenkins 1998). The activation of this pathway has been reported to be involved in plant defense responses (Coram et al. 2008). Some more pathways which help the plant to fight against various types of stresses such as "purine metabolism"; "phenylalanine metabolism"; "thiamine metabolism"; "glutathione metabolism" also showed

Table 1. Number of DEGs compared between PBW343 and FLW29 at different time points of both control and treated sample

Time interval (hpi)	Number of DEGs	Upregulated DEGs	Downregulated DEGs
PBW343_C12 vs FLW29_C12	91	29	62
PBW343_C48 vs FLW29_C48	261	138	123
PBW343_C72 vs FLW29_C72	134	74	60
PBW343_T12 vs FLW29_T12	99	7	92
PBW343_T48 vs FLW29_T48	111	49	62
PBW343_T72 vs FLW29_T72	199	99	100

differential expression in this study (Fig. 3). Studies revealed that purine metabolism involves various enzymes such as phosphatase, kinase, adenyl pyrophosphatase, etc. Thiamine metabolism pathway which involves enzymes such as phosphatase and kinase is also shown to provide better responses in plants against the environmental stresses (Rapala-Kozik et al. 2008).

Domains, families and transcription factors involved with the DEGs

Interproscan was used for the identification of domains and families in differentially expressed genes. As a result of domain search, maximum number of downregulated genes were found to possess WRKY, Bowman-Birk, Anthranilate synthase, Pectinesterase inhibitor and Gnk2-homologous domains. Moreover, the upregulated genes mostly belonged to the glutaredoxin, glutamine amidotransferase, asparagine synthase, asparagine synthase, Redoxin domains (Supplementary Fig. S5). In InterProScan family search, the downregulated genes were found mostly under WRKY, DNA/RNA polymerase, ribonuclease-H, band 7/SPFH domain superfamilies and the upregulated genes were mostly under glutaredoxin, protochlorophyllide reductase, dehydrogenase, asparagine synthase protein families at the early stage of infection. At the later stage of infection, xylanase inhibitor, peptidase, xylanase inhibitor, alpha/beta hydrolase, peptidase C1A and papain-like cysteine endopeptidase families were mainly found (Supplementary Fig. S5).

PlantTFDB was used to identify transcription factors (TF) from transcriptome data. At 12 hpi, MYB was the most abundant of the identified TFs, followed by WRKY, bHLH, MADS, and NAC. Similarly, at 48 hpi, the most abundant TF was GRAS, followed by NAC, Orphans, Tify, Trihelix, AP2-EREBP, WRKY, bHLH, ABI3VP1, C3H, and MYB-related, whereas at 72 hpi, AP2-EREBP, Tify, MADS, SBP, and WRKY were found. Many downstream genes are activated or repressed by TFs, resulting in stress tolerance (Agarwal and Jha 2010). At 12 hpi, we observed WRKY gene expression (WRKY76 and WRKY 45-2) in response to stripe rust infection in FLW29, implying a role for WRKY in pathogen defense and phytohormone signaling functions (Wang et al. 2020). Our study discovered several isoforms of MYB that play critical roles in stress development and adaptation. Basic helix-loop-helix (bHLH) proteins are important regulators in plant defense mechanisms. It activates various types of genes involved in plant response to environmental signals such as hormone signaling. Ethylene responsive factor (AP2/ERF) proteins which dominate at 72 hpi have become the subject of intensive research due to their involvement in

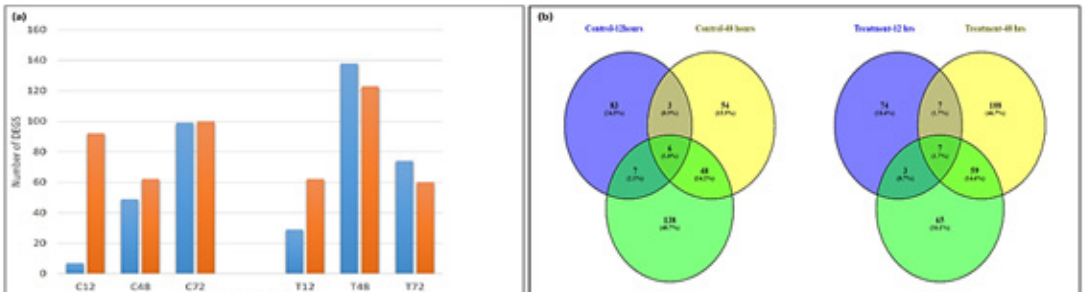

Fig. 1. (a) Regulation of differentially expressed genes between PBW343 and FLW29 and (b) Venn diagram representing number of shared and unique DEGs between PBW343 vs. FLW29 at different time points of control and Psttreated samples

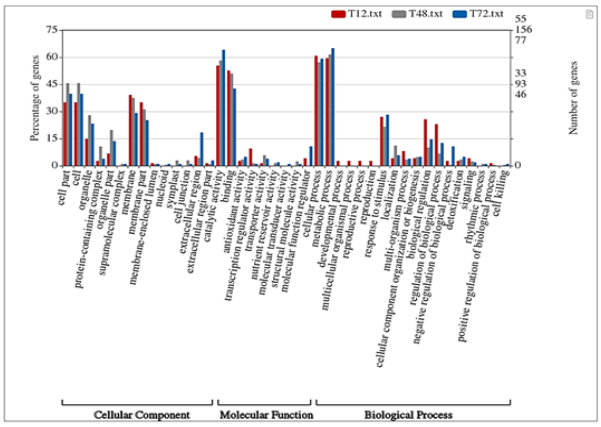

Fig. 2. GO distribution of differentially expressed genes between two NILs involved in biological processes, molecular functions and cellular components at different time points

various biological processes and stress defense mechanisms (Djemal and Khoudi 2015).

Functional analysis of stripe rust infection induced genes using Mapman

Mapman software was used to depict the biotic stress responsive pathways, hormone signaling, transcription factors, and defense related genes. They are related to differentially expressed genes between two NILs of treated condition across three infection intervals (Fig. 4). At 12 hours of infection, two DEGs found to have higher expression in the resistance line, which is related to cell wall degradation and modification associated gene. In the later stage of infection, stress related signaling pathways like Calcium and MAP kinase signaling, receptor kinases such as leucine rich repeat, thaumatin, RLK1, DUF 26, wheat

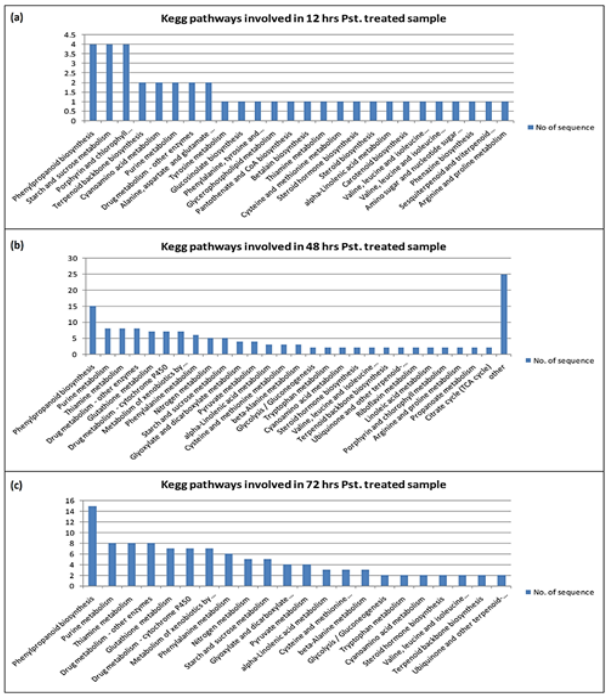

Fig. 3. Comparison of KEGG pathways enriched in the DEGS at (a) 12 hpi, (b) 48 hpi and (c) 72 hpi

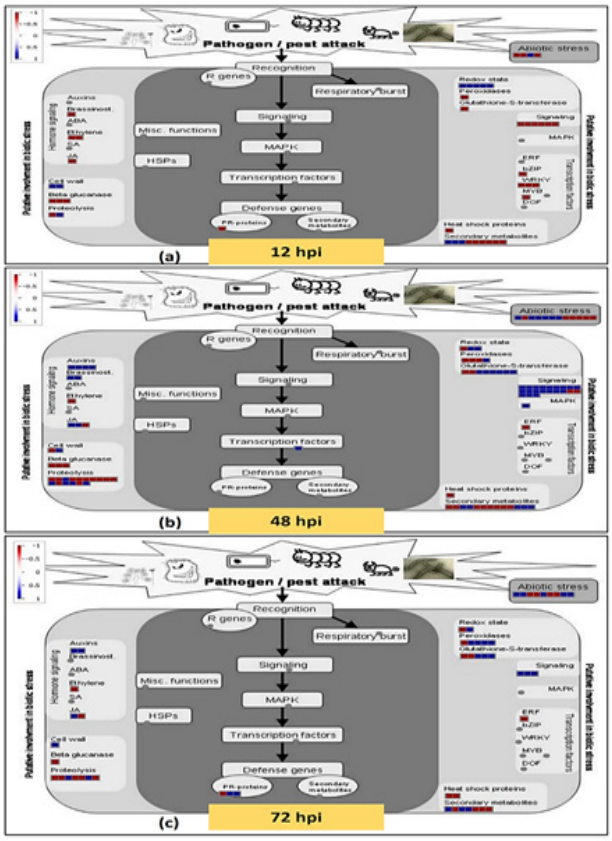

Fig. 4. Mapman visualisation of defense genes response after pathogen attack in both the cultivars

LRK10, crinkly were highly expressed in FLW29 compared to PBW343. The activation of mitogen-activated protein kinases (MAPKs) and calcium-dependent protein kinases (CDPKs), and expression of defense-related genes are among the major responses that occur in biotic stress condition. Under the secondary metabolite pathways, genes playing roles in glucosinolates synthesis, phenylpropanoids, flavonoids, lignin and phytoene synthase pathways were significantly enriched under biotic stress. Furthermore, the stress response pathways showed that the PR-proteins, glutathione-S-transferase, peroxidases, and the genes relating to jasmonate synthesis signaling pathways were enriched in resistant line, FLW29 under disease stress. Also, transcription factors like zinc finger, GRAS, and snf7 were encoded in the highly upregulated DEGs in FLW29.

Protein-protein interaction network

PPI (Protein-Protein Interaction) network visualization analysis was used to identify potential regulators of the DEGs and to predict regulatory relationships. A total of 88 proteins, were involved in the main network based on the STRING database of *T. aestivum* (Fig. 5). Aminomethyl transferase; which belongs to the GcvT family (Traes_2BL_2768AE3B1.1) was the hub protein with the highest degree of 14 that catalyzes the degradation of glycine by the glycine cleavage system. This protein was predicted to interact with the chaperonin (HSP60) family protein that binds RuBisCO small and large subunits and is implicated in the assembly of the enzyme oligomer. The hub protein interacts with the genes that mainly codes for cysteine synthase, asparagine synthetase, phenylalanine ammonia-lyase family, pathogenesis-related protein 1-15, WRKY domain. Moreover, the hubgene interacting proteins belongs to protein kinase, ATP-synt_D, serine/threonine protein kinase, and peroxidase family. Furthermore, the proteins

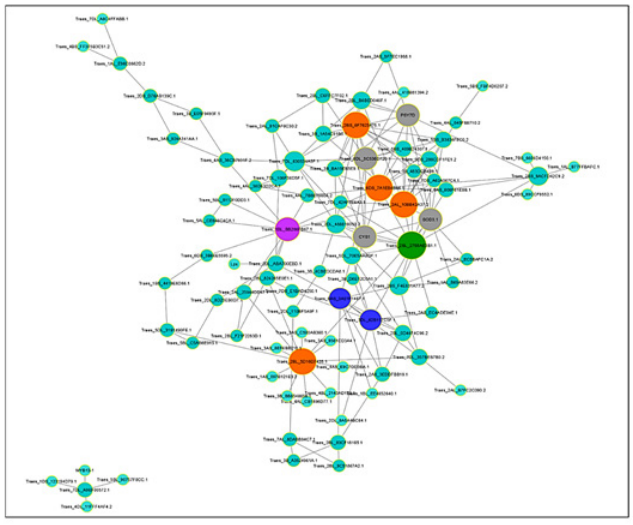

Fig. 5. Protein-protein interaction (PPI) network of the DEGs

encoding for phenylalanine ammonia-lyase (PAL), MYB13-1, lipoxygenase, cysteine synthase, phytoene synthase has also been found to interact with the hub gene in this network, which are all reported to play a very crucial role in the plant defense mechanism against pathogens (Chen et al. 2017; Karthikeyan et al. 2005; Romero et al. 2014).

The present study aimed to identify differentially expressed genes in wheat leaf tissues to decipher associated enzymes, pathways, and transcriptional factors associated with wheat stripe rust through transcriptional profiling. Differentially expressed transcripts with LRR, Zinc finger, GRAS domain, and a number of other plant resistance genes, including serine/threonine-protein kinase, chitinases, peroxidases, mitogen-activated protein kinases (MAPKs), calcium-dependent protein kinases (CDPKs), and PR proteins, were more abundant in FLW29 than in PBW343. Differentially expressed MYB and WRKY transcription factor genes have also been found to mediate multiple stress tolerance in plants during the early stages of infection. In addition, the pathways explored by KEGG and Mapman are involved in wheat defense mechanisms to biotic stresses and contribute to the ability of the plant to inhibit fungal growth and development. These pathways can be useful for further investigation to elucidate the crop's stress improvement and develop effective strategies for breeding resistant wheat varieties to obtain a better control of stripe rust.

Supplementary material

Supplementary Tables S1 and S2; Supplementary Figs. S1 to S5 are presented and can be access online www.isgpb.org.

Authors' contribution

Conceptualization of research (GM, DCM); Designing of the experiments (GM, DCM); Contribution of experimental materials (SCB); Execution of field/lab experiments and data collection (DC); Analysis of data and interpretation (PD, MG); Preparation of the manuscript (AKS, SK, SCB, KKC, AR).

References

Agarwal P.K and Jha B. 2010. Transcription factors in plants and ABA dependent and independent abiotic stress signalling. Biol.Plant., **54**: 201–212.

Altschul S.F., Gish W., Miller W., Myers E.W. and Lipman, D.J. 1990. Basic local alignment search tool. J. Mol Biol., **215**: 403–410.

Andrews S. 2010. FastQC: a quality control tool for high throughput sequence data. Available online at: http://www.bioinformatics.babraham.ac.uk/projects/fastqc

Bolger A.M., Lohse M. and Usadel B. 2014. Trimmomatic: a flexible trimmer for Illumina sequence data. Bioinformatics,**30**: 2114–2120.

Chen W., Wellings C., Chen X., Kang Z. and Liu T. 2014. Wheat stripe (yellow) rust caused by *Puccinia striiformis* f. sp. *tritici*. Mol. Plant Pathol., **15**: 433–446.

Chen X.M. 2005. Epidemiology and control of stripe rust [*Puccinia striiformis f. sp. tritici*] on wheat. Canadian J. Plant Pathol., **27**: 314–337.

Chen Y., Li F., Tian L., Huang M., Deng R., Li X., Chen W., Wu P., Li M., Jiang H. and Wu G. 2017. The Phenylalanine Ammonia Lyase Gene LjPAL1 Is Involved in Plant Defense Responses to Pathogens and Plays Diverse Roles in Lotus japonicus-Rhizobium Symbioses. Mol. Plant Microbe Interact., **30**: 739–753.

Conesa A., Götz S., García-Gómez J.M., Terol J., Talón M. and Robles M. 2005. Blast2GO: a universal tool for annotation, visualization and analysis in functional genomics research. Bioinformatics, **21**: 3674–3676.

Coram T.E., Settles M.L. and Chen X. 2008. Transcriptome analysis of high-temperature adult-plant resistance conditioned by Yr39 during the wheat-*Puccinia striiformis* f. sp. *tritici*interaction. Mol. Plant Pathol., **9**: 479–493.

Djemal R. and Khoudi H. 2015. Isolation and molecular characterization of a novel WIN1/SHN1 ethylene-responsive transcription factor TdSHN1 from durum wheat (*Triticum turgidum*. L. subsp. *durum*). Protoplasma, **252**: 1461–1473.

Dodds P.N. and Rathjen J.P. 2010. Plant immunity: towards an integrated view of plant-pathogen interactions. Nat. Rev. Genet., **11**: 539–548.

Franceschini A., Szklarczyk D., Frankild S., Kuhn M., Simonovic M., Roth A., Lin J., Minguez P., Bork P., von Mering C. and Jensen L.J. 2013. STRING v9.1: protein-protein interaction networks, with increased coverage and integration. Nucleic Acids Res., **41**: D808-815.

Goff L. A., Trapnell C. and Kelley D. (2012).CummeRbund: visualization and exploration of Cufflinks high-throughput sequencing data. R package version, 2(0).

Gupta P.K., Kumar J., Mir R.R. and Kumar A. 2009. Marker-Assisted Selection as a Component of Conventional Plant Breeding. Plant Breed. Rev., **33** 145-217.

Jin J., Tian F., Yang D.C., Meng Y.Q., Kong L., Luo J. and Gao G. 2017. PlantTFDB 4.0: toward a central hub for transcription factors and regulatory interactions in plants. Nucleic Acids Res., **45**: D1040–D1045.

Kanehisa M. and Goto S. 2000. KEGG: kyoto encyclopedia of genes and genomes. Nucleic Acids Res., **28**: 27–30.

Karthikeyan M., Jayakumar V., RadhikaK., Bhaskaran R., Velazhahan R. and Alice D. 2005. Induction of resistance in host against the infection of leaf blight pathogen (Alternaria palandui) in onion (Allium cepa var aggregatum). Indian J. Biochem. Biophys., **42**: 371–377.

Pawar S.K., Sharma D., Duhan J.S., Saharan M.S., Tiwari R. and Sharma I. 2016. Mapping of stripe rust resistance QTL in Cappelle–Desprez × PBW343 RIL population effective in northern wheat belt of India. 3 Biotech., **6**: 76.

Rapala-Kozik M., Kowalska E. and Ostrowska K. 2008. Modulation of thiamine metabolism in Zea mays seedlings under conditions of abiotic stress. J.Exp. Bot., **59**: 4133–4143.

Romero L.C., Aroca M.Á., Laureano-Marín A.M., Moreno I., García I. and Gotor C. 2014. Cysteine and cysteine-related signaling pathways in *Arabidopsis thaliana*. Mol. Plant., **7**: 264–276.

Shannon P., Markiel A., Ozier O., Baliga N.S., Wang J.T., Ramage D., Amin N., Schwikowski B. and Ideker T. 2003. Cytoscape: a software environment for integrated models of biomolecular interaction networks. Genome Res., **13**: 2498–2504.

Thimm O., Bläsing O., Gibon Y., Nagel A., Meyer S., Krüger P., Selbig J., Müller L.A., Rhee S.Y. and Stitt M. 2004. mapman: a user-driven tool to display genomics data sets onto diagrams of metabolic pathways and other biological processes. Plant J., **37**: 914–939.

Trapnell C., Pachter L. and Salzberg S.L. 2009. TopHat: discovering splice junctions with RNA-Seq. Bioinformatics,**25:** 1105–1111.

Trapnell C., Williams B.A., Pertea G., Mortazavi A., Kwan G., van Baren M.J., Salzberg S.L., Wold B.J. and Pachter L. 2010. Transcript assembly and quantification by RNA-Seq reveals unannotated transcripts and isoform switching during cell differentiation. Nat. Biotechnol., **28**: 511–515.

Wabila C., Neumann K., Kilian B., Radchuk V. and Graner A. 2019. A tiered approach to genome-wide association analysis for the adherence of hulls to the caryopsis of barley seeds reveals footprints of selection. BMC Plant Biol., **19**: 95.

Wang H., Zou S., Li Y., Lin F. and Tang D. 2020. An ankyrin-repeat and WRKY-domain-containing immune receptor confers stripe rust resistance in wheat. Nat Commun., **11**: 1353. 15139-6

Wang X., Basnayake B.M.V.S., Zhang H., Li G., Li W., Virk N., Mengiste T. and Song F. 2009. The Arabidopsis ATAF1, a NAC Transcription Factor, Is a Negative Regulator of Defense Responses Against Necrotrophic Fungal and Bacterial Pathogens. MPMI., **22**: 1227–1238.

Weisshaar B. and Jenkins G.I. 1998. Phenylpropanoid biosynthesis and its regulation. Curr. Opin. Plant Biol., 1: 251–257.

Ye J., Fang L., Zheng H., Zhang Y., Chen J., Zhang Z., Wang Jing, Li S., Li R., Bolund L. and Wang J. 2006. WEGO: a web tool for plotting GO annotations. Nucleic Acids Res., **34**: W293–W297.

Zhang J., Zhang P., Dodds P. and Lagudah E. 2020. How Target-Sequence Enrichment and Sequencing (TEnSeq) Pipelines Have Catalyzed Resistance Gene Cloning in the Wheat-Rust Pathosystem. Front. Plant Sci., **11**.

Supplementary Table S1. Summary of data output quality generated by RNA-seq library

Sample_name	Total_length(bp)	Raw_Reads	Clean reads	Q20	GC content
FLW29_C12_1	3209739956	21256556	17213957	97.11	56
FLW29_C12_2	3214203516	21286116	16405018	97.08	55
FLW29_C12_3	4977881850	33185879	20809439	96.56	55
FLW29_T12_1	3843817344	25455744	21540764	97.17	52
FLW29_T12_2	3532328051	23392901	18854033	97.08	55
FLW29_T12_3	4125667050	27504447	22675040	96.58	54
FLW29_C48_1	2858678697	18931647	14046884	97.25	54
FLW29_C48_2	3228697704	21382104	15372485	96.54	52
FLW29_C48_3	3517247250	23448315	13586886	96.71	55
FLW29_T48_1	2819788496	18674096	15751323	96.8	55
FLW29_T48_2	3038268886	20120986	14953229	94.85	54
FLW29_T48_3	3630921900	24206146	18905493	97.79	57
FLW29_C72_1	4691275500	31275170	12335040	96.93	55
FLW29_C72_2	3271770150	21811801	13936157	96.75	57
FLW29_C72_3	3438044550	22920297	15609376	96.56	59
FLW29_T72_1	3814890300	25432602	16759359	97.29	58
FLW29_T72_2	3824763300	25498422	16037136	95.33	57
FLW29_T72_3	3697082250	24647215	15618145	96.93	57
PBW343_C12_1	3793209996	25120596	19321511	97.03	53
PBW343_C12_2	3437461999	22764649	18867750	96.75	55
PBW343_C12_3	3070751850	20471679	12221662	96.8	58
PBW343_T12_1	3609344393	23902943	18753237	97.12	55
PBW343_T12_2	2576179290	17060790	13728156	97.26	55
PBW343_T12_3	4523106900	30154046	21423482	97.12	57
PBW343_C48_1	2810047637	18609587	11893910	97.39	55
PBW343_C48_2	2025913546	13416646	9396276	97.75	53
PBW343_C48_3	3055026900	20366846	15837614	97.45	55
PBW343_T48_1	3413179236	22603836	16962679	96.81	53
PBW343_T48_2	1137479527	7532977	5856688	97.39	55
PBW343_T48_3	4709403000	31396020	25185317	96.9	57
PBW343_C72_1	4703747100	31358314	23596443	96.93	57
PBW343_C72_2	4409618700	29397458	19497104	96.9	56
PBW343_C72_3	3677173650	24514491	16588666	96.75	58
PBW343_T72_1	4715553600	31437024	22416796	96.81	57
PBW343_T72_2	4549023300	30326822	18912976	95.64	59
PBW343_T72_3	4298551050	28657007	20853807	96.37	59

Supplementary Table S2. Summary statistics of alignment reads of FLW29 and PBW343 over the reference genome

Time interval	Condition	Left read alignment		Right read alignment		Overall alignment
		Mapped once	Multiple times	Mapped once	Multiple times	
FLW29						
12 hours	Control	31649239 (76.0%)	6363035 (20.1%)	31349783 (75.3%)	6300088 (20.1%)	75.60%
	Treatment	53267279 (82.7%)	15196935 (28.5%)	52930531 (82.2%)	15113185 (28.6%)	82.50%
48 hours	Control	30356419 (81.8%)	6501309 (21.4%)	30070325 (81.0%)	6437464 (21.4%)	81.40%
	Treatment	40026787 (83.4%)	9025148 (22.5%)	39502110 (82.3%)	8898411 (22.5%)	82.80%
72 hours	Control	49151594 (82.4%)	12788519 (26.0%)	48554467 (81.4%)	12583362 (25.9%)	81.90%
	Treatment	51171403 (82.3%)	23656262 (46.2%)	50697391 (81.5%)	23440860 (46.2%)	81.90%
PBW343						
12 hours	Control	46113870 (81.60%)	8688415 (18.8%)	45448607 (80.4%)	8539387 (18.8%)	81.00%
	Treatment	50180817 (83.2%)	9876127 (19.7%)	49517757 (82.1%)	9726061 (19.6%)	82.70%
48 hours	Control	34195797 (79.5%)	6560202 (19.2%)	33907377 (78.8%)	6515259 (19.2%)	79.20%
	Treatment	40783766 (82.2%)	6498902 (15.9%)	40242936 (81.1%)	6406799 (15.9%)	81.70%
72 hours	Control	32560160 (77.7%)	8639096 (26.5%)	32154255 (76.8%	8521343 (26.5%)	77.30%
	Treatment	34278421 (70.8%)	11066710 (32.3%)	34034197 (70.3%)	10973159 (32.2%)	70.50%

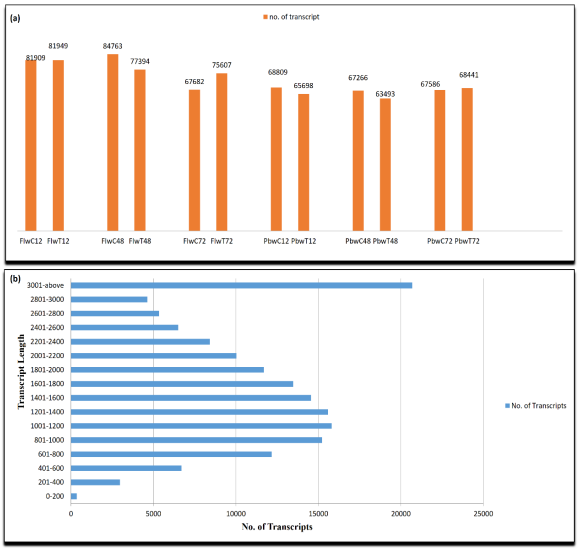

Supplementary Fig. S1. (a) Number of assembled transcripts generated by Cufflinks of FLW29 and PBW343 lines of *Triricum aestivum* under control and treated conditions on different time points and (b) Sequence length distribution of transcriptome assembly of Triricum aestivum.

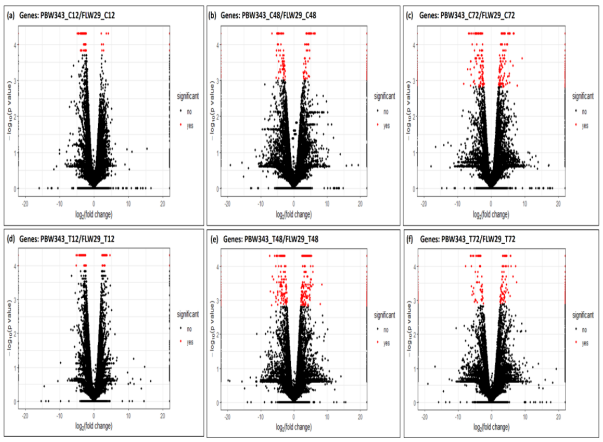

Supplementary Fig. S2. Volcano Plot representing the DEGs between PBW343 and FLW29 of Pst. inoculated samples at different time points based on the log fold change vs –log (p value). The middle of each volcano has two lines which represents the fold change ranges from -20 to 20, while both the sides indicate down-regulation (negative values) and up-regulation (positive values), respectively. The black dots depict non-significant DEGs and the red dots represent significant (up and down regulated) log2fold change to the criteria of (P<0.05 and log2fold change 2 viz., untreated DEGs at (a) 12hrs, (b) 48hrs and (c) 72hrs. DEGs after Pst treatment at (d) 12hrs, (e) 48 hrs and (f) 72hrs

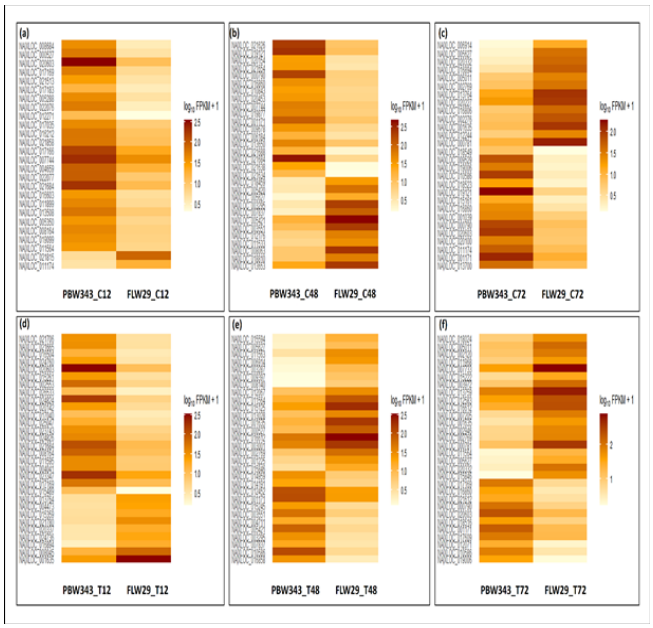

Supplementary Fig. S3. Heatmap representing the DEGs between PBW343 and FLW29 of control sample at (a) 12 hrs, (b) 48 hrs, (c) 72 hrs and Pst inoculated samples at (d) 12 hrs, (e) 48 hrs and (f) 72 hrs based on log2 FPKM values of the first 30 highly expressed DEGs. The dark color on expression matrix represents upregulated genes and light color represents downregulated genes

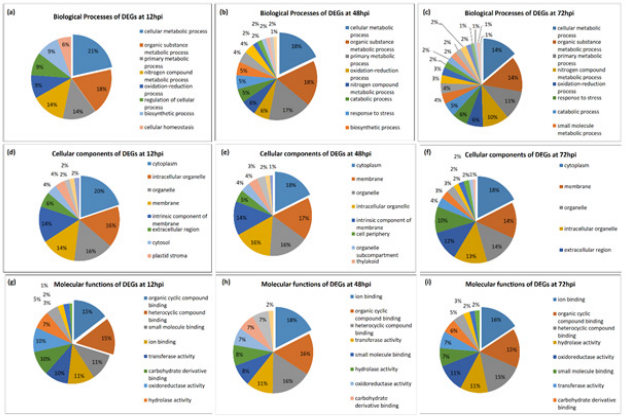

Supplementary Fig. S4. Pie chart depicting percentage of DEGs involved in different biological processes at (a) 12 hrs, (b) 48 hrs, (c) 72 hrs; cellular components at (d) 12 hrs, (e) 48 hrs, (f) 72 hrs and molecular functions at (g) 12 hrs, (h) 48 hrs, (i) 72 hrs

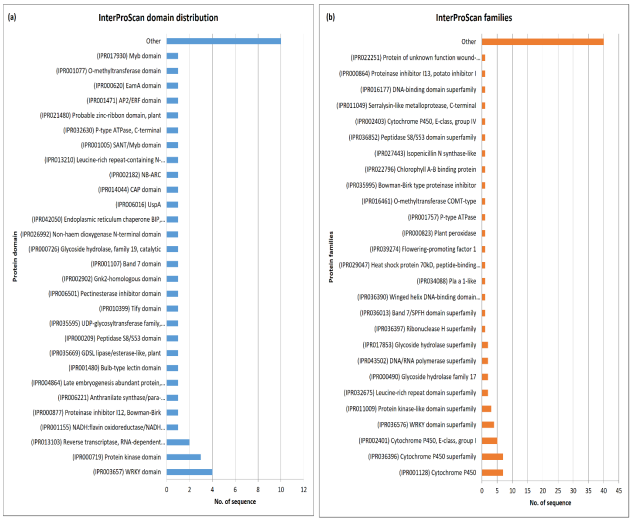

Supplementary Fig. S5. List of number of genes involved in (a) protein domains and (b) families at 12hpi